HYPERON STAR*

Ilona Bednarek

Institute of Physics, University of Silesia
Uniwersytecka 4, 40-007, Katowice, Poland

(Received October 29, 2009)

The extended nonlinear model has been applied to construct neutron star matter equation of state. In the case of neutron star matter with non-zero strangeness the extension of the vector meson sector by the inclusion of nonlinear mixed terms results in the stiffening of the equation of state and accordingly in the higher value of the maximum neutron star mass.

PACS numbers: 97.60.Jd, 26.60.Dd, 26.60Kp, 26.60.–c

1. Introduction

At the core of a neutron star the matter density ranges from a few times the density of normal nuclear matter (ρ_0) to about an order of a magnitude higher. At such densities exotic forms of matter such as hyperons are expected to emerge. The appearance of these additional degrees of freedom and their impact on a neutron star structure have been the subject of extensive studies [1–4].

The analysis of the role of strangeness in nuclear structure in the aspect of multi-strange system is of great importance for both nuclear physics and for astrophysics. In the latter case understanding the properties of hyperon star is still a relevant item. In the core of a neutron star, in the very high density environment, there is also the possibility for strange gravitational phenomena [5].

Recent results of neutron star mass measurements with the most spectacular and promising one, obtained for neutron star–white dwarf binary system, with the Arecibo radio telescope, suggest that the maximum neutron star mass is rather high [6]. According to original observations, the mentioned above binary system, includes a neutron star with the largest mass ever reported M(PSR J0751+1807) $= 2.1 \pm 0.2\ M_{\odot}(1\sigma)$ [7]. However,

* Presented at the XXXIII International Conference of Theoretical Physics, "Matter to the Deepest", Ustroń, Poland, September 11–16, 2009.

this result has been corrected down to the new value 1.26 $M_\odot$ with the estimated errors 1.12–1.30 $M_\odot(1\sigma)$ and 0.98–1.53 $M_\odot(2\sigma)$ [8, 9]. This reversed value of the mass has been obtained on the basis of the improved value of the orbital decay and the detection of the Shapiro delay.

The most accurately measured neutron star masses come from observations of the radio binary pulsars. These reliably determined neutron star masses are in the range 1.5–1.65 $M_\odot$. The largest mass obtained recently from the analysis of timing observations of the pulsar PSR J1903+0327 has been estimated at the value of 1.7 ± 0.4 $M_\odot$. This is the largest precisely known neutron star mass. There are other reported results of measurements of neutron star masses which indicate their high values. Among others there are observations of pulsars in globular clusters: the pulsar PSR B1516+02B located in the globular cluster M5 with estimated value of the mass $1.96^{+0.09}_{-0.12}$ $M_\odot$, pulsar PSR J1748-2021B in the globular cluster NGC 6440 with the median mass of 2.74 ± 0.21 $M_\odot$. However, these results are rather uncertain. Another examples of the high neutron star masses include compact star in the low mass X-ray binary (LMXB) 4U 1636-536 with the mass estimated at the value of 2.0 ± 0.1 $M_\odot$ [10] or the X-ray source EXO 0748-676 which has been constrained by the detection of gravitational redshift of certain absorption lines. In the latest case the obtained results combined with other observational data lead to individually estimated mass and radius of the star at the value of $M \geq 2.10 \pm 0.28$ $M_\odot$ and $R \geq 13.8 \pm 1.8$ km [11, 12].

Besides the measurements of neutron star masses also the estimated value of the radius of the isolated neutron star RX J1856.5-3754 [13] indicates its high value of the mass. The analysis of thermal emission from the star surface allows the determination of the ratio of the photospheric radius R_∞ to the distance d. This result together with the assumed model of the atmosphere support the large value of radius of the star $R > 12$ km.

Nuclear matter in neutron star interiors represents environments with extremely high value of the isospin asymmetry f_a which defines the neutron excess in the system $f_a = (\rho_n - \rho_p)(\rho_n + \rho_p)$, ρ_n and ρ_p represent neutron and proton densities, respectively. The sum $\rho_n + \rho_p = \rho_b$ defines the baryon density. The equation of state (EOS) of neutron-rich matter can be approximated by the following parabolic formula $\epsilon(\rho_b, f_a) = \epsilon(\rho_b, 0) + S_2(\rho_b) f_a^2$, where $\epsilon(\rho_b, f_a)$ is the energy per particle of asymmetric infinite nuclear matter.

The EOS includes the symmetric matter contribution which does not depend on the isospin asymmetry $\epsilon(\rho_b, 0)$ and the symmetry energy term $S_2(\rho_b)$. The last one totally determines the isospin dependence of the system.

The most important characteristics of a neuron star, namely its maximum mass and the typical neutron star radius are strictly connected with the form of the equation of state involved, but as the maximum mass is

controlled by stiffness of the EOS, the radius is determined by the density dependence of the symmetry energy $S_2(\rho_b)$. The presented above results of astrophysical observations which suggest high value of neutron star masses should be compared with the data obtained from terrestrial nuclear experiments [14].

The reported results from the elliptic flow in the heavy ion collisions are used to constrain the symmetric part of nuclear matter EOS. Basing on the analysis of the flow data and the results from transport calculations the values of pressure in the density range $2 < \rho_b/\rho_0 < 4.6$ have been estimated [14]. On the other hand, the density dependence of the symmetry energy is still poorly known. Data from intermediate energy heavy ion reactions, which include subthreshold kaon production, constrain the form of the symmetry energy in the density range $(2 < \rho_b/\rho_0 < 3)$. The one-parameter fit to the low-density behavior of the symmetry energy has been introduced, where $u = \rho/\rho_0$ and J is the symmetry energy coefficient equal to $S_2(\rho_0)$. This dependence also allows one to determine the transition density ρ_t between the crust and the core of a neutron star. The constraints on the value of γ_t, for the transition density ρ_t, obtained from the intermediate-energy heavy-ion collisions provides the range $\gamma_\mathrm{t} \sim 0.69$–$1.05$ [15–17].

In general, heavy ion experiments support the soft EOS, at moderate densities. The considerable stiffening of the EOS is indispensable for higher densities in order to reproduce the observed high value of neutron star masses. Thus, the combined current astrophysical and heavy-ion constraints lead to a very specific form of the EOS which in the case of non-strange nuclear matter is satisfactorily reproduced by many models. However, there is a contradiction between the very high value of the observed neutron star masses and the EOS of strangeness-rich nuclear matter. In general, the appearance of hyperons in neutron star interiors is connected with the substantial softening of the EOS and this results in the low value of the maximum mass.

2. The model

Vector densities, which are defined by the value of the vector meson fields, are the decisive factors that contribute to the EOS of dense matter in neutron star interiors. The construction of the extended vector meson sector has been done by the inclusion the fourth-order self-interaction term of the vector mesons. Different forms of the SU(3) invariants have been included. This allows one to take into account divers nonlinear vector meson interaction terms. This results in the appearance of various nonlinear vector meson couplings, among which there are terms which relate the strange and non-strange mesons. As a consequence strong connections between the asymmetry and strangeness fraction of the model have emerged. For details concerning the model considered see the paper [18].

The Lagrangian function of the system consists of a baryonic part which includes the full octet of baryons together with terms describing interaction of baryons with scalar and vector mesons, and a mesonic part. The mesonic part contains also additional interactions between mesons. The most general form of the Lagrangian function can be written as follows

$$\mathcal{L} = \sum_B \bar{\psi}_B i\gamma^\mu D_\mu \psi_B - \sum_B m_B(\sigma,\sigma^*)\overline{\psi}_B\psi_B + \mathcal{L}_M\,, \tag{1}$$

where baryon fields $\Psi_B^T = (\psi_N, \psi_\Lambda, \psi_\Sigma, \psi_\Xi)$ are composed of the following isomultiplets [1]:

$$\Psi_N = \begin{pmatrix}\psi_p\\ \psi_n\end{pmatrix}, \qquad \Psi_\Lambda = \psi_\Lambda\,,$$

$$\Psi_\Sigma = \begin{pmatrix}\psi_{\Sigma^+}\\ \psi_{\Sigma^0}\\ \psi_{\Sigma^-}\end{pmatrix}, \quad \Psi_\Xi = \begin{pmatrix}\psi_{\Xi^0}\\ \psi_{\Xi^-}\end{pmatrix},$$

D_μ is the covariant derivative of baryons which in terms of ω_μ, ρ_μ^a and ϕ_μ fields is given by

$$D_\mu = \partial_\mu + ig_{\omega B}\omega_\mu + ig_{\phi B}\phi_\mu + ig_{\rho B}I_{3B}\tau^a\rho_\mu^a\,. \tag{2}$$

The meson part of the Lagrangian function

$$\begin{aligned}\mathcal{L}_M \;=\; & \tfrac{1}{2}\partial_\mu\sigma\partial^\mu\sigma + \tfrac{1}{2}\partial_\mu\sigma^*\partial^\mu\sigma^* - U_{\text{eff}}\left(\sigma,\sigma^*,\omega_\mu,\rho_\mu^a,\phi_\mu\right)\\ & -\tfrac{1}{4}\Omega_{\mu\nu}\Omega^{\mu\nu} - \tfrac{1}{4}R_{\mu\nu}^a R^{a\mu\nu} - \tfrac{1}{4}\Phi_{\mu\nu}\Phi^{\mu\nu}\end{aligned} \tag{3}$$

includes the field tensors $\Omega_{\mu\nu}, \Phi_{\mu\nu}$ and $R_{\mu\nu}^a$ defined as $\Omega_{\mu\nu} = \partial_\mu\omega_\nu - \partial_\nu\omega_\mu$, $\Phi_{\mu\nu} = \partial_\mu\phi_\nu - \partial_\nu\phi_\mu$ and $R_{\mu\nu}^a = \partial_\mu\rho_\nu^a - \partial_\nu\rho_\mu^a$. All meson interaction terms are collected in the potential function which can be written as a sum of linear and nonlinear parts, respectively

$$\mathcal{U}_{\text{eff}}\left(\sigma,\sigma^*,\omega_\mu,\rho_\mu^a,\phi_\mu\right) = \mathcal{U}_{\text{lin}}\left(\sigma,\sigma^*,\omega_\mu,\rho_\mu^a,\phi_\mu\right) + \mathcal{U}_{\text{nl}}\left(\sigma,\sigma^*,\omega_\mu,\rho_\mu^a,\phi_\mu\right)\,. \tag{4}$$

The linear scalar and vector meson part of the potential takes the form

$$\begin{aligned}\mathcal{U}_{\text{lin}}\left(\sigma,\sigma^*,\omega_\mu,\rho_\mu^a,\phi_\mu\right) \;=\; & \tfrac{1}{2}m_\sigma^2\sigma^2 + \tfrac{1}{2}m_{\sigma^*}^2\sigma^{*2} - \tfrac{1}{2}m_\omega^2\left(\omega_\mu\omega^\mu\right)\\ & -\tfrac{1}{2}m_\rho^2(\rho_\mu^a\rho^{\mu a}) - \tfrac{1}{2}m_\phi^2\left(\phi_\mu\phi^\mu\right)\,,\end{aligned} \tag{5}$$

whereas its nonlinear part is given by

$$\begin{aligned}\mathcal{U}_V \;=\; & \tfrac{1}{4}c_3(\rho_\mu^a\rho^{\mu a})^2 + \tfrac{3}{4}c_3(\rho_\mu^a\rho^{\mu a})(\phi_\nu\phi^\nu) + \tfrac{1}{8}c_3(\phi_\mu\phi^\nu)^2\\ & +\tfrac{3}{4}c_3(\phi_\mu\phi^\mu)(\omega_\nu\omega^\nu) + \tfrac{1}{4}(g_\rho g_\omega)^2\Lambda_V(\phi_\mu\phi^\mu)^2\\ & +\tfrac{1}{4}c_3(\omega_\mu\omega^\mu)^2 - \tfrac{1}{2}(g_\rho g_\omega)^2\Lambda_V(\rho_\mu^a\rho^{\mu a})(\phi_\nu\phi^\nu)\\ & +(g_\rho g_\omega)^2\Lambda_V(\rho_\mu^a\rho^{\mu a})(\omega_\nu\omega^\nu) - \tfrac{1}{2}(g_\rho g_\omega)^2\Lambda_V(\phi_\mu\phi^\mu)(\omega_\nu\omega^\nu)\,.\end{aligned} \tag{6}$$

Calculations performed in this paper are based on the standard TM1 parameter set [19]. The inclusion of the mixed nonlinear isoscalar–isovector coupling Λ_V provides the possibility of modifying the high density dependence of the symmetry energy and requires the adjustment of the $g_{\rho N}$ coupling constant to keep the same value of the symmetry energy at saturation. Thus, in the isovector sector the parameters $g_{\rho N}$ and Λ_V have been fitted to reproduce the symmetry energy coefficient at the value $J = 36.89$ MeV. The remaining ground state properties are left unchanged.

Vector mesons–hyperon coupling constants are taken from the quark model. Whereas the scalar couplings $g_{\sigma B}$ of the Λ, Σ and Ξ hyperons require constraining in order to reproduce the estimated values of the potential felt by a single Λ, Σ and Ξ in the saturated nuclear matter. The knowledge about the hyperon–hyperon interaction is also indispensable. The coupling of hyperons to the strange meson σ^* has been limited by the estimated value of hyperon potential depths in hyperon matter and this has direct consequences for neutron star parameters. Recent experimental data [20] indicate a much weaker strength of hyperon–hyperon (Y–Y) interaction. The strong Y–Y interaction is related to the value of the potential $U_\Lambda^{(\Lambda)} = -20$ MeV, whereas the weak one corresponds to $U_\Lambda^{(\Lambda)} = -5$ MeV [20, 21].

3. Results and discussion

The integration of the Tolman–Oppenheimer–Volkov (TOV) equations with a specific equation of state leads to the mass-radius relation and allows one to determine the value of the maximum mass which in a sense can give a measure of the impact of particular nonlinear couplings between vector mesons.

In Fig. 1 the equations of state obtained for different cases of nonlinear potentials presented in this paper have been shown. Extreme, dashed curves represent results obtained for the standard TM1 parameterization, for the non-strange and strangeness rich matter, respectively. The case when the matter includes only nucleons and leptons gives the stiffest EOS whereas the directly opposed result namely the softest EOS can be obtained for the standard TM1 parameterization extended by the inclusion of hyperons. Other equations of state presented in this figure aim to provide the analysis of the influence of additional vector meson nonlinear interaction. The cases $\Lambda_V = 0.008$ and $\Lambda_V = 0.01$ have been taken into account. The obtained results indicate for the strong tendency for stiffening of the EOS for the increasing value of the parameter Λ_V. The inclusion of nonlinear vector meson interactions has profound consequences for the structure of neutron stars and this can be deduced from Fig. 2 where the mass-radius relations for the obtained equations of state have been shown. Dotted curves depict

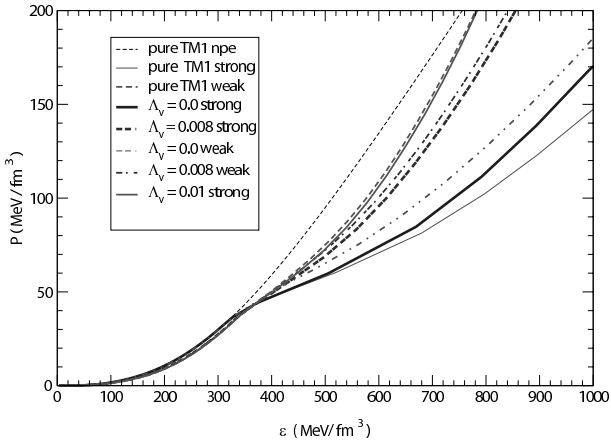

Fig. 1. The EOS obtained for the nonlinear models. The EOSs for the nonlinear models with different values of the parameter Λ_V are included. All parameters that enter the considered models are taken from [18].

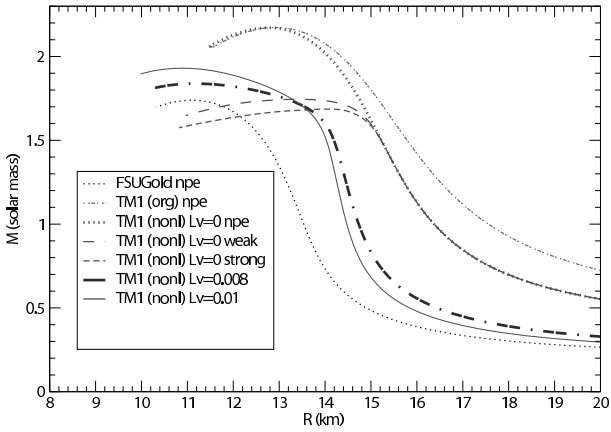

Fig. 2. The mass-radius relations obtained for the chosen models.

the results calculated for non-strange matter. The mass-radius relation for the FSU Gold parameter set has been given, for comparison. The maximum mass increases with increasing value of the parameter Λ_V, giving in the results neutron star models with masses exceeding 2 $M_\odot$ and with reduced radii. Thus, one can expect that solutions with nonlinear vector meson couplings lead to neutron star models with substantially greater density. The mass-radius diagram includes the cases for non-strange and strange matter. Changing the value of the parameter Λ_V solutions with substantially reduced value of the transition density have been obtained [18]. This points

to the conclusion that the crust-core boundary moves to lower density region leading to the models with reduced value of the non-homogenous phase. It has been shown that in the very nonlinear models the inclusion of hyperons does not soften the EOS; on the contrary, it leads to its considerable stiffening. The consequences for neutron star parameters are straightforward and appear as a considerable growth of neutron star masses. Thus one of the inevitable conclusions is that in the case of nonlinear models the inclusion of hyperons does not result in the lowering of a neutron star mass. This is of special interest when considering reported astrophysical data which indicate large neutron star masses.

REFERENCES

[1] N.K. Glendenning, *Astrophys. J.* **293**, 470 (1985); *Compact Stars*, Springer–Verlag, New York 1997.

[2] I. Bednarek, R. Manka, *Int. J. Mod. Phys.* **D10**, 607 (2001).

[3] F. Weber, *Pulsars as Astrophysical Laboratories for Nuclear and Particle Physics*, IOP Publishing, Philadelphia 1999.

[4] J. Schaffner-Bielich, A. Gal, *Phys. Rev.* **C62**, 034311 (2000).

[5] J. Sladkowski, *Int. J. Mod. Phys.* **D9**, 311 (2001).

[6] I. Sagert, M. Wietoska, J. Schaffner-Bielich, Ch. Sturm, *J. Phys. G* **35**, 014053 (2008).

[7] D.J. Nice, E.M. Splaver, I.H. Stairs, O. Lohmer, A. Jessner, M. Kramer, J.M. Cordes, *Astrophys. J.* **634**, 1242 (2005).

[8] D. Blaschke, T. Klahn, F. Sandin, *J. Phys. G* **35**, 014051 (2008).

[9] D. Nice, 40 Years of Pulsars, Montrea 2007, conference contribution.

[10] D. Barret, J.F. Olive, M.C. Miller, *Mon. Not. R. Astron. Soc.* **361**, 855 (2005).

[11] J. Cottam, F. Paerles, M. Mendez, *Nature* **420**, 51 (2002).

[12] F. Ozel, *Nature* **441**, 1115 (2006).

[13] J.E. Trümper, V. Burvitz, F. Haberl, V.E. Zavlin, *Nucl. Phys. Proc. Suppl.* **B132**, 560 (2004).

[14] P. Danielewicz, R. Lacey, W.G. Lynch, *Science* **298**, 1592 (2002).

[15] Bao-An Li, L.W. Chen, C.M. Ko, *Phys. Rep.* **464**, 113 (2008).

[16] J. Piekarewicz, M. Centelles, *Phys. Rev.* **C79**, 054311 (2009).

[17] M. Centelles, X. Roca-Maza, X. Vinas, M. Warda, *Phys. Rev. Lett.* **102**, 122502 (2009).

[18] I. Bednarek, R. Manka, *J. Phys. G* **36**, 095201 (2009).

[19] Y. Sugahara, H. Toki, *Prog. Theor. Phys.* **92**, 803 (1994).

[20] H. Takahashi *et al.*, *Phys. Rev. Lett.* **87**, 212502 (2001).

[21] H.Q. Song, R.K. Su, D.H. Ku, W.L. Qian, *Phys. Rev.* **C68**, 055201 (2003).